Influence of forward rake and skew blade angle on positive slope characteristics of mixed flow pumps

IOP Conf. Series: Earth and Environmental Science **240** (2019) 032045 doi:10.1088/1755-1315/240/3/032045

Influence of forward rake and skew blade angle on positive slope characteristics of mixed flow pumps

N Nitta [1], S Maeda [1], H Kanno [1], K Miyagawa [2], Y Shinozuka [3], K Kado [3], and S Tomimatsu [3]

[1] Department of Applied Mechanics, Waseda University, Tokyo, 169-8555, Japan
[2] Department of Applied Mechanics and Aerospace Engineering, Waseda University, Tokyo, 169-8555, Japan
[3] R&D Center, DMW Corporation, Miyoshi, Mishima, Shizuoka, 411-8560, Japan

naruki.soccer03@toki.waseda.jp

Abstract. In many of the mixed flow pumps that have been studied in the past, the impeller has a sweepback wing. Especially, the positive slope characteristics have been studied to operate pump in a stable regime. The cause of the positive slope in the characteristic curve of the mixed flow pump is the reverse flow, with the turning becomes stronger, at the leading edge of the blade tip side in the flow rate range. Also, at the flow rate at which the slope of the characteristic curve becomes positive, the angular momentum becomes negative at the leading edge of the impeller, and the work amount sharply decreases at the leading edge more than the work amount increase at the trailing edge so the angular momentum decreases. However, the influence of the forward rake and skew blade on the performance, the positive slope characteristics, and the internal flow have not been studied much. In this study, we designed and analysed a forward rake and skew blade mixed flow pump. About the forward rake and skew blade, we found the cause of the positive slope characteristics is the same reason as the sweepback wing, but the flow rate range of occurrence of the positive slope characteristics was lower in the forward rake and skew pump than in the sweepback pump.

Introduction There are various instability phenomena in turbomachinery. The positive slope characteristic of the performance curve at the low flow rate region of a high specific speed pump such as a mixed flow pump may cause the instability flow characteristics depending on the resistance curve. If the unstable characteristics occurs, surging and turning stall may be induced. Surges are self-excited vibrations caused by strongly periodic fluctuation of the discharge pressure and flow rate during pump operation. The turning stall occurs if the blade has a small attack angle when operating in the low flow rate range, and a stall region occurs on a blade. In that state, since the flow path is closed, the attack angle of the blade on the suction side is increased, and the stall transfers to the adjacent blade. However, the blade in stalling recovers and the stall region propagates in the direction of lift of the blade cascade. This phenomenon causes severe pressure pulsation, which may cause fatigue fracture due to repeated loads acting on the blades. So it is very important to control the positive slope characteristics in order to obtain stable operation.
In many of the mixed flow pumps that have been studied in the past, the impeller has a sweepback wing. However, the influence on the performance, the positive slope characteristics, and the internal flow about the forward rake and skew blade have not been studied much. In this study, we designed a forward

rake and skew blade mixed flow pump, and compared its performance and the internal flow of the conventional mixed flow pump and forward rake and skew blade mixed flow pump using CFD analysis. Furthermore, we examined the cause of the positive slope characteristics and how the forward rake and skew influences the performance.

1. Designed method and analysis of the forward rake and skew blade mixed flow pump

The method of designing the forward rake and skew pump (FRAS pump) was the leading edge of the impeller tip side was lengthened towards the upstream at the tip side as shown in figure 1. Table 1 shows both mixed flow pumps specification. Figure 2 shows meridional shape.

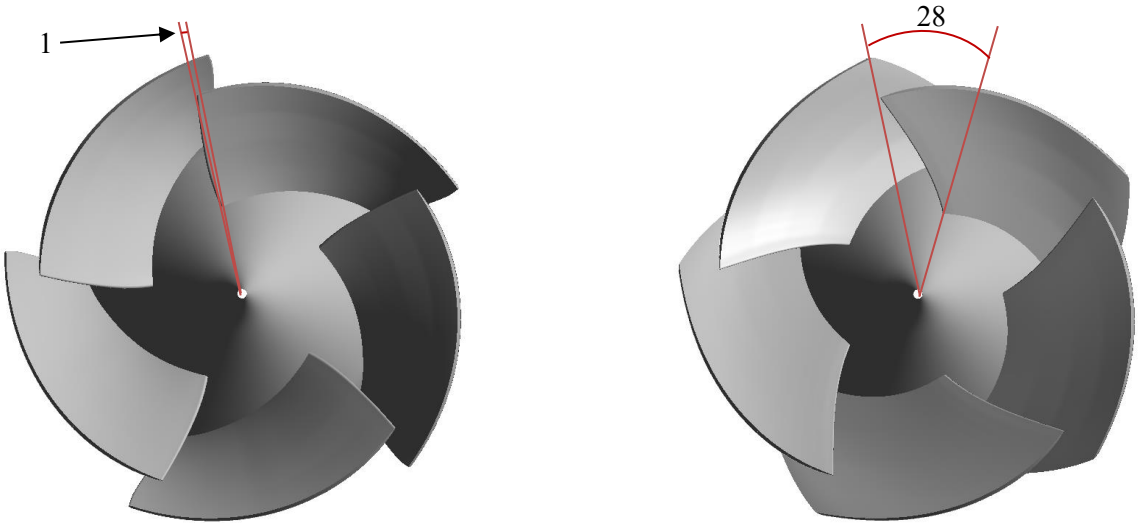

(a) Conventional pump**.**

(b) Forward rake and skew pump (FRAS pump).

Figure 1. Impeller shapes.

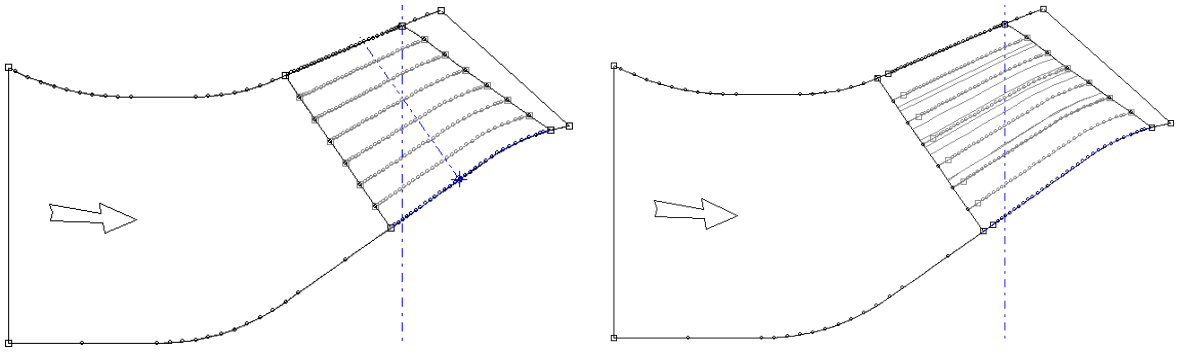

(a) Conventional pump. (b) FRAS pump.

Figure 2. Meridional shape.

Table 1. Pump specification.

	Conventional	FRAS	
Number of impeller blade	5		
Number of diffuser blade	7		
Impeller diameter at inlet (tip)	253.6		mm
Impeller diameter at outlet (tip)	299.4		mm
Skew angle	1	28	deg

The domain of the numerical simulation is shown in figure 3. Figure 4 shows a detailed view of the mesh lines in impeller and diffuser, and Table 2 shows the detailed mesh information. The numerical meshes were generated by TurboGrid. ANSYS CFX 17.2 was used for the numerical simulation. Steady state computation using the Reynolds-Averaged Navier-Stokes equation (RANS) was performed with the SST k-ω (Shear Stress Transport) turbulence model. The analysis was performed using periodic boundaries, with the total pressure applied at the inlet and the mass flow rate applied at the outlet. The rotational region and static region were connected with a mixing plane interface.

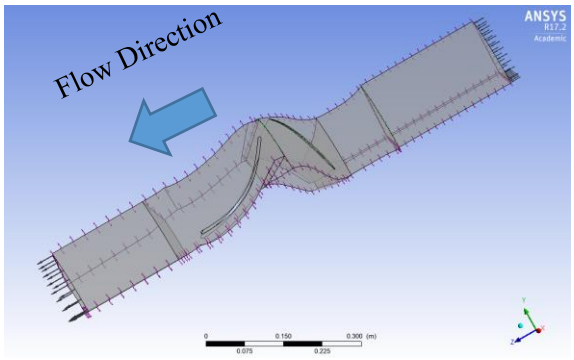

Figure 3. View of computational domain.

Table 2. Detailed mesh information.

Flow domains	Number of nodes
Inblock	71269
Impeller	836355
Diffuser	777689
Total	1685313

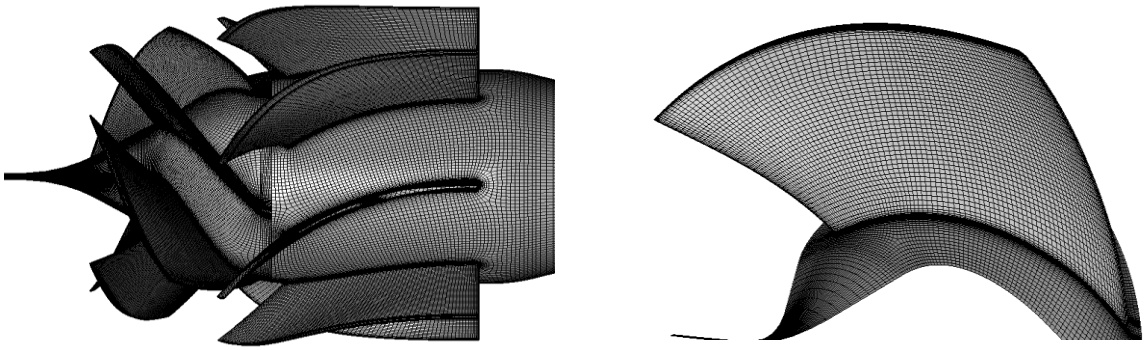

Figure 4. Mesh configuration in pump (left) and blade of impeller (right).

2. Pump performance

Figure 5 shows the computational results of the pump performance for the conventional pump and the FRAS pump. The positive slope characteristics at the flow rate coefficient is observed at $Q/Q_{bep} = 0.545\sim0.636$ in the conventional pump, on the other hand, in the FRAS pump at the flow rate coefficient $Q/Q_{bep} = 0.364\sim0.455$.

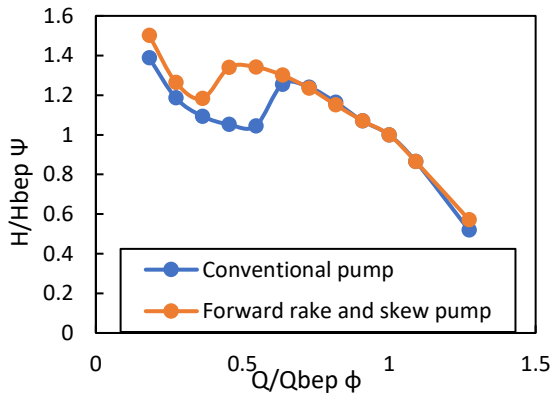

(a) Head coefficient.

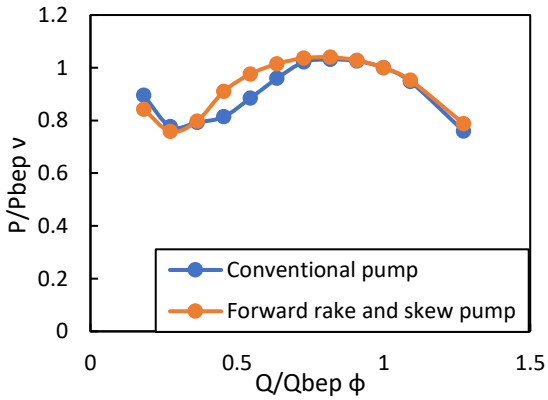

(b) Shaft power coefficient.

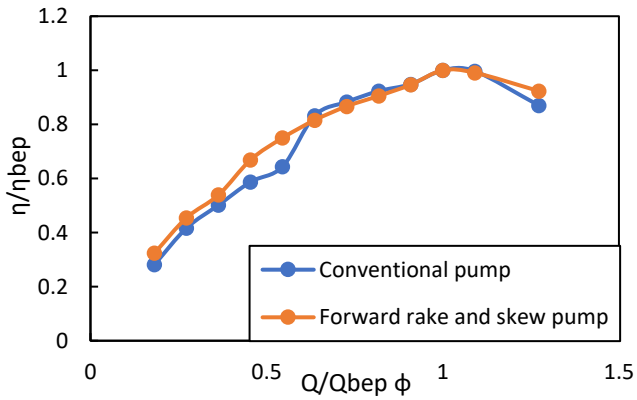

(c) Efficiency.

Figure 5. Pump performance at each operating point.

3. The positive slope characteristics

3.1. Loss of the impeller

Figure 6 shows the loss coefficient distribution of impeller inlet at the leading edge in the intervals $Q/Q_{bep} = 0.545,0.636$ for the conventional pump and figure 7 shows it for the FRAS pump. For the conventional pump the loss was larger at the tip side of its impeller inlet at $Q/Q_{bep} = 0.545$ than at $Q/Q_{bep} = 0.636$. For the FRAS pump, it was not large at tip side of its impeller inlet at $Q/Q_{bep} = 0.545, 0.636$. The loss coefficient is defined as

$$\mathrm{I} = \mathrm{i} + \frac{1}{2}w^2 - \frac{1}{2}U^2 \tag{1}$$

$$\zeta = \frac{(I_1 - I)}{\frac{1}{2}U_1^2} \tag{2}$$

Where i, *w*, *U,* are static enthalpy, relative velocity, and rotational velocity. The subscript 1 means the entrance to the impeller. This equation quotes the swirling flow characteristic equation of Bernoulli's law. When there is no loss, the rothalpy is constant. In other words, when there is a loss, the difference of rothalpy is not 0. Therefore, the loss factor ζ means that there is a local loss.

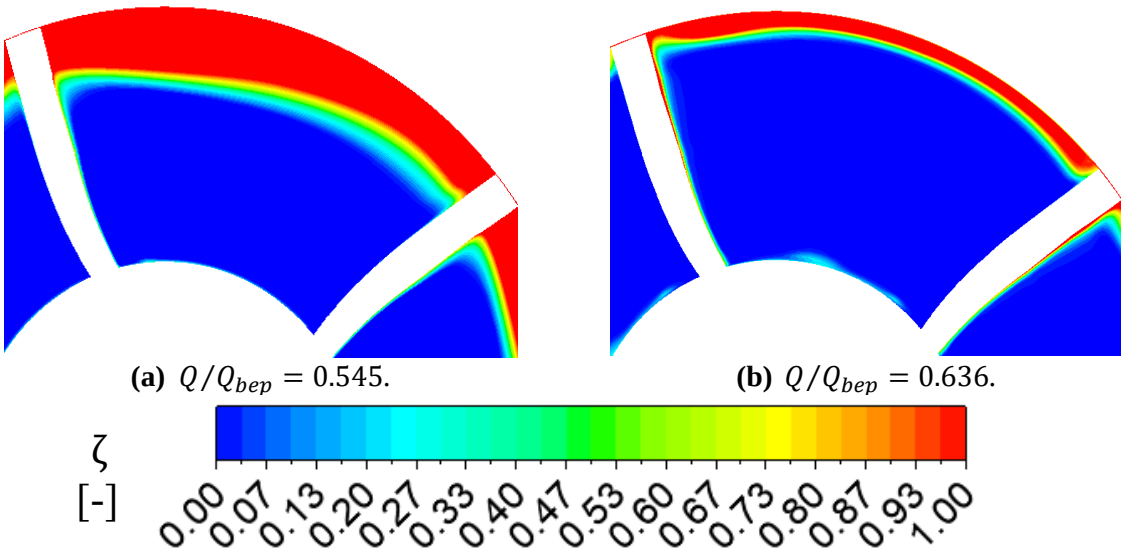

(a) $Q/Q_{bep} = 0.545$. **(b)** $Q/Q_{bep} = 0.636$.

Figure 6. Loss coefficient distribution of impeller inlet about the conventional pump.

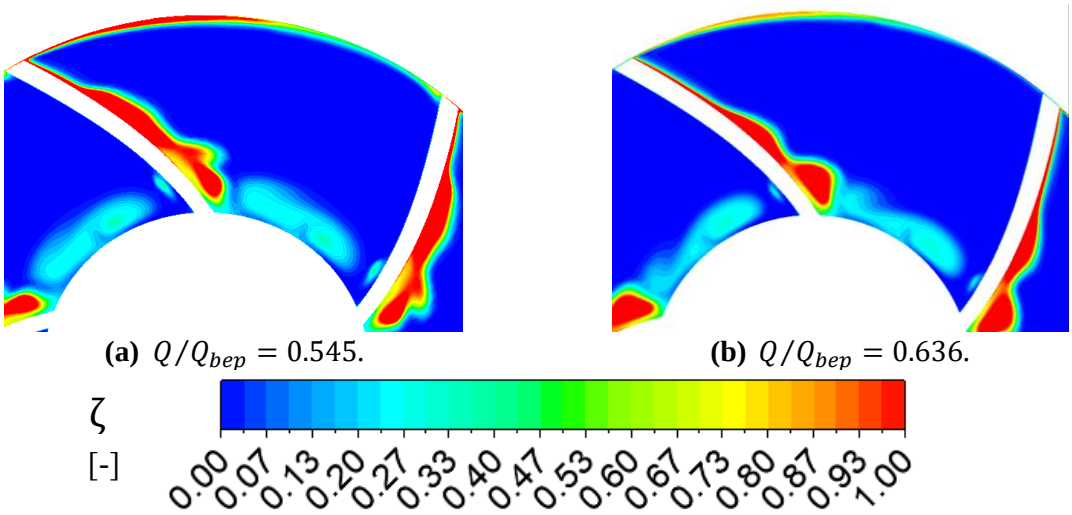

(a) $Q/Q_{bep} = 0.545$. **(b)** $Q/Q_{bep} = 0.636$.

Figure 7. Loss coefficient distribution of impeller inlet about the FRAS pump.

3.2. The reverse flow

Figure 8 shows the flow velocity ratio ($= V_m/U_2$)profile of the meridional plane in the range $Q/Q_{bep} = (0.545, 0.636)$ of the conventional pump and figure 9 shows it of the FRAS pump. For the conventional pump the reverse flow occurred at the tip side of its impeller inlet at $Q/Q_{bep} = 0.545$ but didn't occur at $Q/Q_{bep} = 0.636$. For the FRAS pump it occurred at tip side of its impeller inlet at $Q/Q_{bep} = 0.545, 0.636$. So, the larger loss coefficient was accompanied by the reverse flow, which caused the pump head decrease.

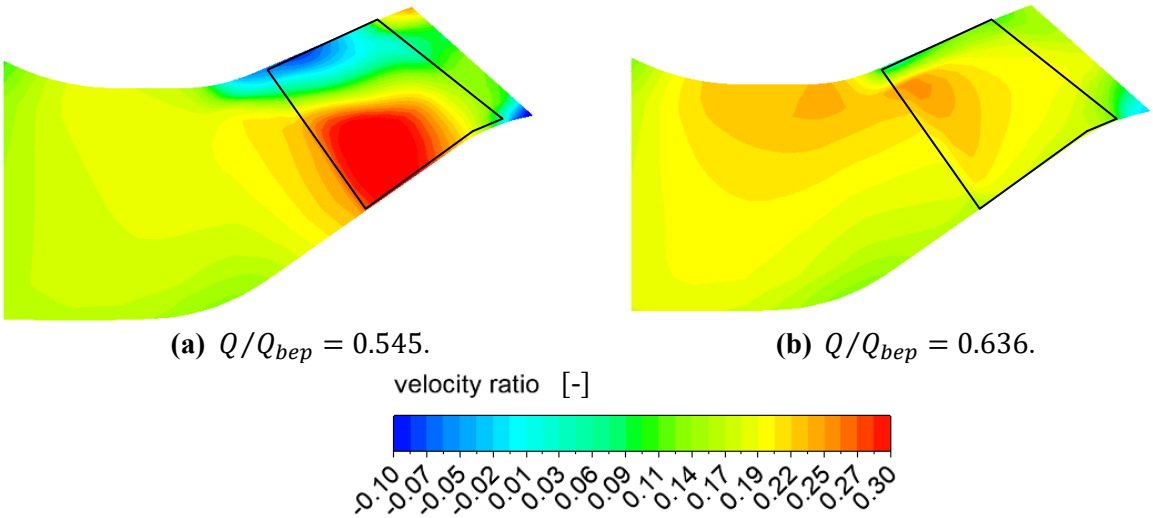

(a) $Q/Q_{bep} = 0.545$. **(b)** $Q/Q_{bep} = 0.636$.

Figure 8. Flow profile in the meridional plane of the conventional pump.

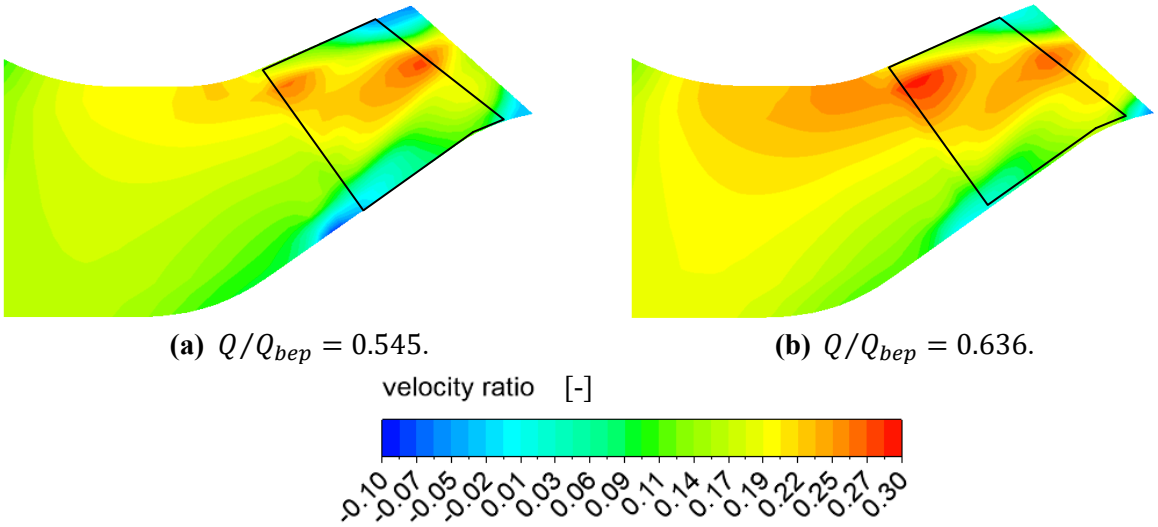

(a) $Q/Q_{bep} = 0.545$. **(b)** $Q/Q_{bep} = 0.636$.

Figure 9. Flow profile of the meridional plane about the FRAS pump.

3.3. The vortex

Figure 10 shows the loss distribution by the vortex in the range $Q/Q_{bep} = (0.545, 0.636)$ of the conventional pump and figure 11 shows it of the FRAS pump. About the conventional pump, at $Q/Q_{bep} = 0.545$, there was vortex at the tip side of the impeller but at $Q/Q_{bep} = 0.636$, it disappeared. Also, for the FRAS pump, it didn't occur at $Q/Q_{bep} = 0.545, 0.636$. So, the reverse flow was caused by the vortex at the tip side. The Q-criterion is defined as

$$Q = \frac{1}{2}\left(||\Omega||^2 - ||S||^2\right) \tag{3}$$

Where Q, Ω, S, are Q-criterion, vorticity tensor, and rate of strain tensor.

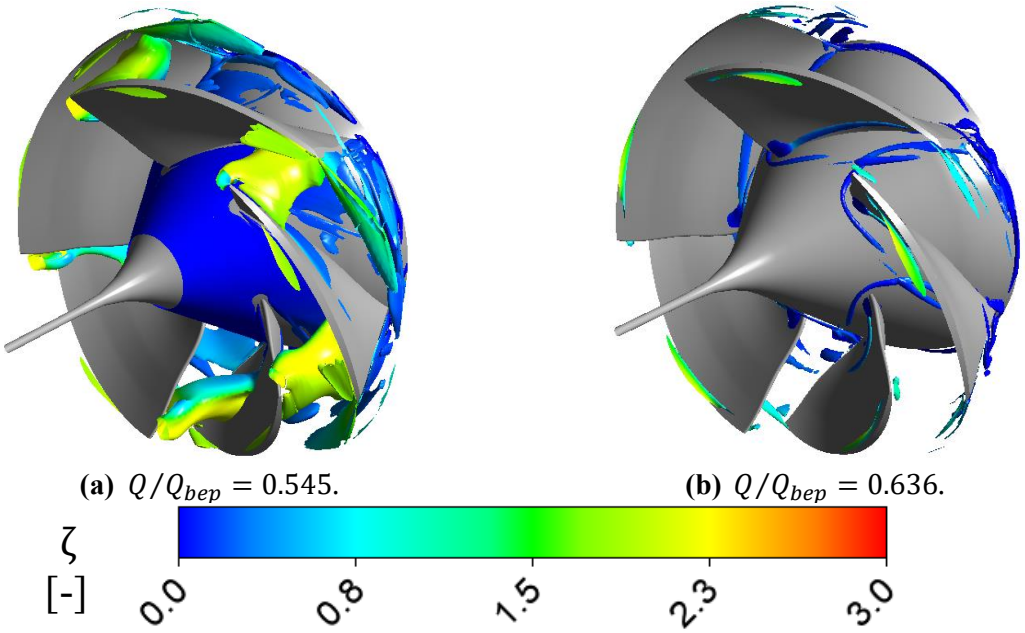

(a) $Q/Q_{bep} = 0.545$. **(b)** $Q/Q_{bep} = 0.636$.

Figure 10. The vortex of the conventional pump.

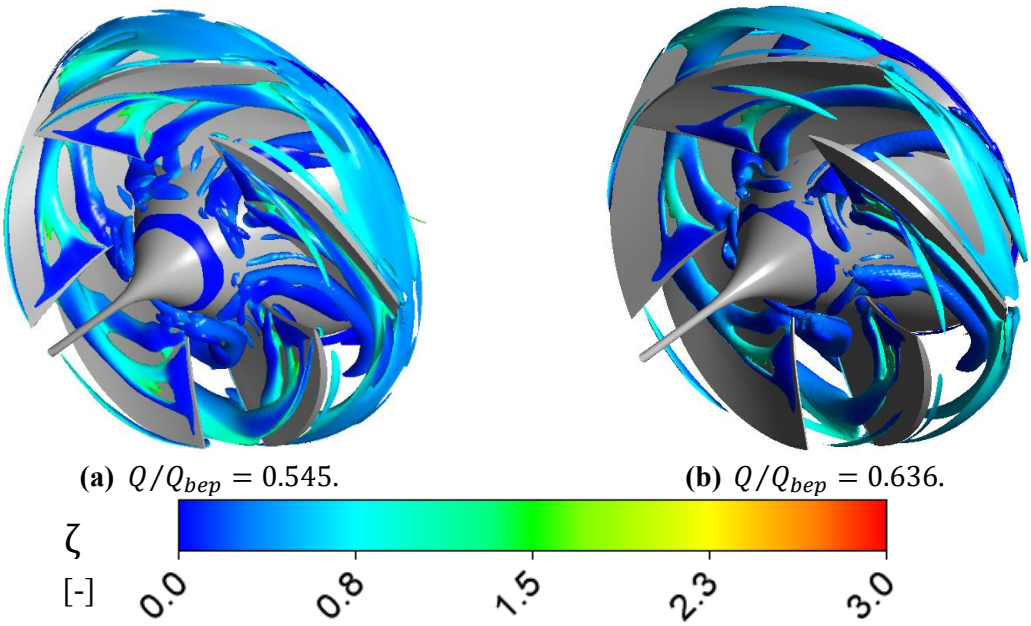

Figure 11. The vortex of the FRAS pump.

3.4. The reverse flow

Figure 12 shows the flow line on the blade at $Q/Q_{bep} = 0.364, 0.545, 0.636$ about the conventional pump and the FRAS pump. About the conventional pump, at $Q/Q_{bep} = 0.364, 0.545$, there was swirling flow on the blade but at $Q/Q_{bep} = 0.636$, it didn't occur. Also, for the FRAS pump, at $Q/Q_{bep} = 0.364$, there was it but at $Q/Q_{bep} = 0.545, 0.636$, it didn't occur. So, the flow along the blade surface at the tip side was disturbed by this swirling flow. Therefore, the vortex appeared at this area.

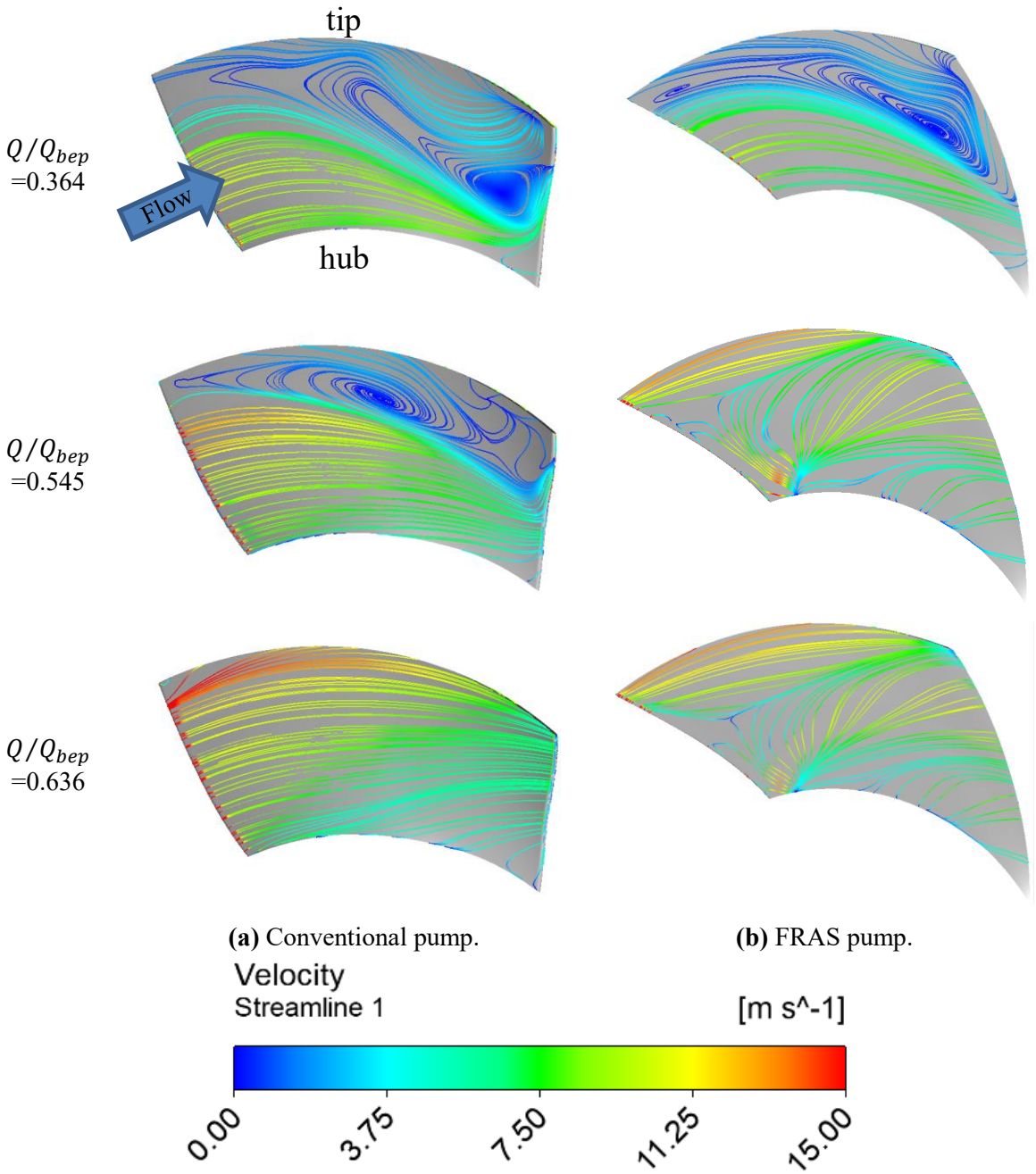

(a) Conventional pump. **(b)** FRAS pump.

Figure 12. The flow line on the blade.

3.5. The port diameter

The port diameter ratio from hub to tip about the conventional pump and the FRAS pump is shown in figure 13. This graph shows that the port diameter ratio increased because of the changing skew angle in the FRAS pump. Especially, this ratio at the tip side was much bigger. So, a large port diameter decreased the swirling flow likelihood.

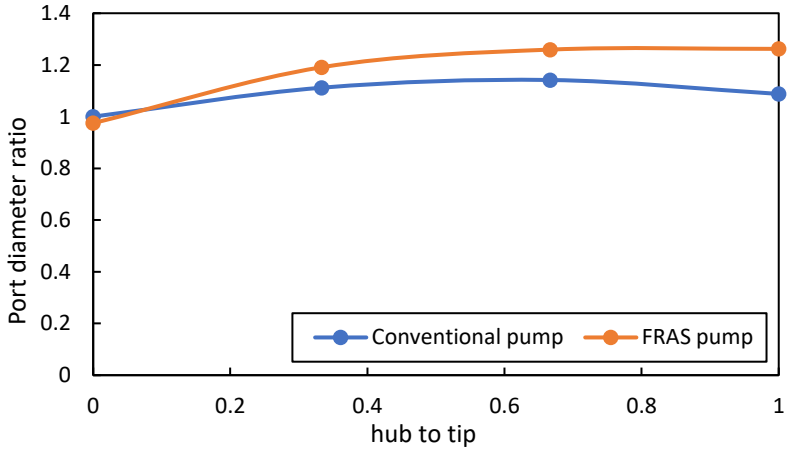

Figure 13. The port diameter.

3.6. Meridional velocity and blade loading distribution

Figure 14 shows that the meridional velocity at $Q/Q_{bep} = 0.545, 0.636$ about the conventional pump and the FRAS pump. These graph show that the less flow at tip side in the conventional pump but larger in the FRAS pump. Figure 15 shows that the blade loading distribution at the tip side from leading edge to trailing edge. At $Q/Q_{bep} = 0.636$, the blade loading on the tip side was large about both pumps but at $Q/Q_{bep} = 0.545$, it was small for the conventional pump. Therefore, the amount of work increased at the tip side of the impeller in the low flow rate region, as a result of the port diameter became larger by changing skew angle. The blade loading coefficient C_p is defined as

$$C_p = P_s/(P_{tout} - P_{tin}) \quad (4)$$

Where P_s is static pressure, P_{tout} is total pressure at outlet of the impeller, P_{tin} is total pressure at inlet of the impeller.

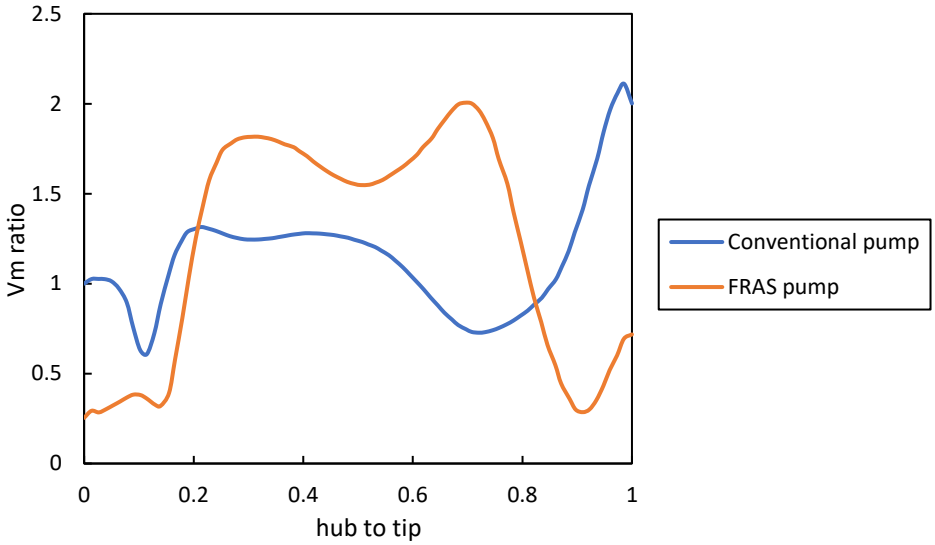

(a) $Q/Q_{bep} = 0.545$.

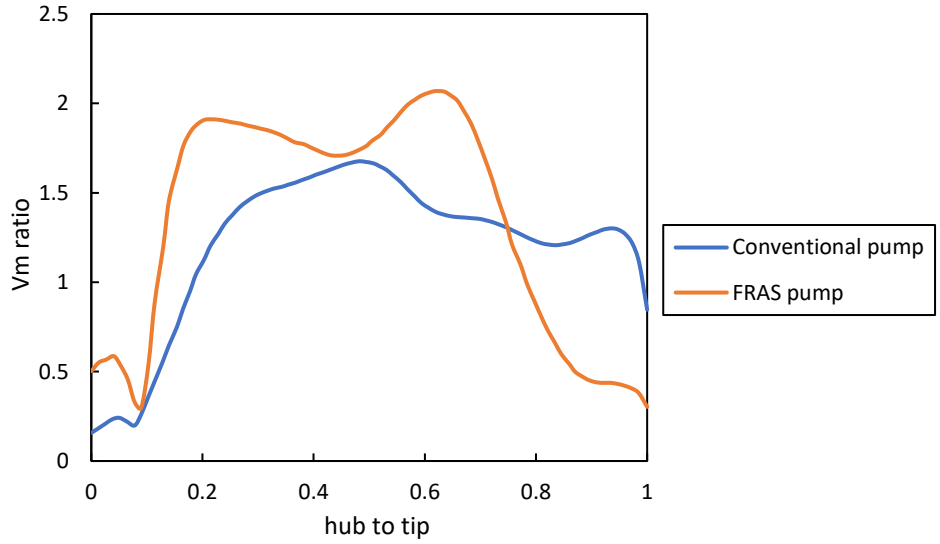

(b) $Q/Q_{bep} = 0.636$.

Figure 14. The meridional velocity.

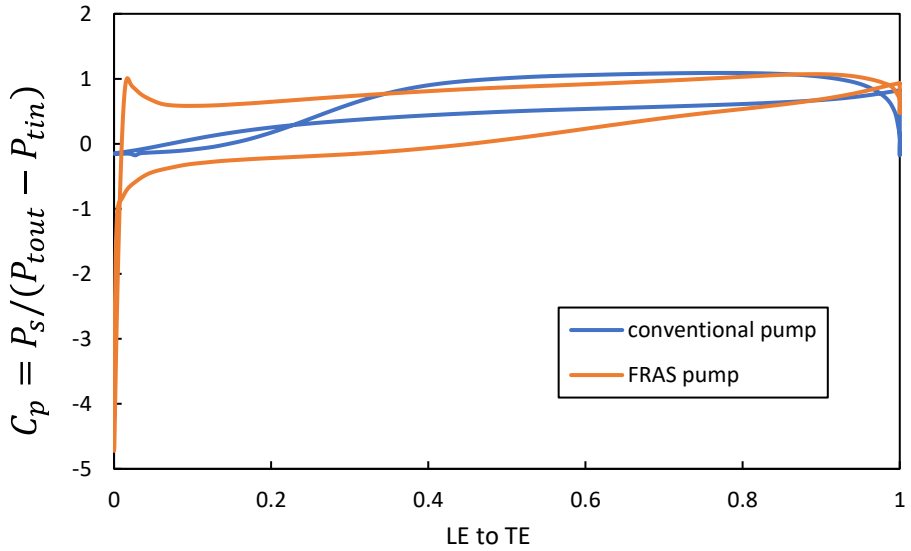

(a) $Q/Q_{bep} = 0.545$.

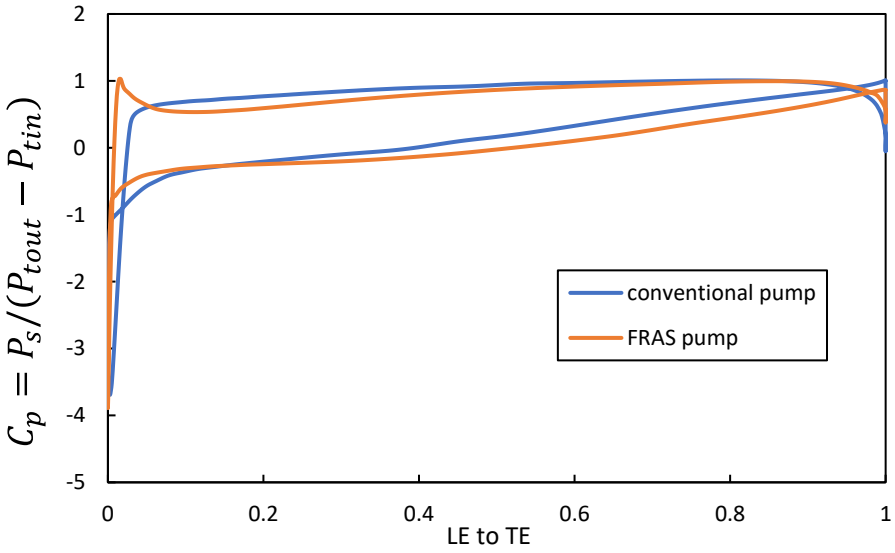

(b) $Q/Q_{bep} = 0.636$.

Figure 15. The blade loading distribution at tip side.

4. Conclusions

(1) The amount of work increased at the tip side of the impeller in the low flow rate region by changing skew angle.
(2) The flow rate ratio of the positive slope region of the Q-H characteristics shifted to low range.

Acknowledgement

The authors would like to thank the Waseda Research Institute for Science and Engineering (WISE) for providing support to the presented research, in context of the project: 'High performance and high reliability research for hydraulic turbomachinery systems'.

References

[1] I Hagiya, C Kato, Y Yamade, T Nagahara, and M Fukaya 2015 Cause specification of performance curve instability in mixed-flow pump by LES *Transactions of the JSME 2016* (Vol.82, No.834)

[2] M Aoki , and A Goto 1994 Positively Sloped Head-Flow Characteristics and Inlet Recirculation of a Mixed-Flow Pump *Transactions of the JSME 1995* (Vol.62, No.596)

[3] Y Nishi, J Fukutomi, and S Nakamura 2013 Study on Instability Characteristics of a Mixed-Flow Pump of Different Blade Loading Distribution near the Blade Tip *Transactions of the JSME 2013* (Vol.79, No.801)

[4] K Kado, D Yamaguchi, and T Kanemoto 2015 Effects of Blade Load on Cavitation Performance for Mixed Flow Pumps *The 13th Asian International Conference on Fluid Machinery* (AICFM13-155)

[5] Y Sekino, and Y Tanabe 2011 Numerical Analysis of Design and Off-design Performance of High Specific Speed Mixed Flow Pumps *Proceedings of the ASME-JSME-KSME 2011 Joint Fluids Engineering Conference* (AJK2011-06051 by JSME)

[6] Y Takayama, and H Watanabe 2009 Multi-objective Design Optimization of a Mixed-Flow Pump *Proceedings of the ASME 2009Fluids Engineering Division Summer Meeting* (FEDSM2009-78348. 2009 by ASME)